Magnetic structure of dysprosium in epitaxial Dy films and in Dy/Er superlattices

K. Dumesnil, C. Dufour, Ph. Mangin, and G. Marchal
Laboratoire Métallurgie Physique et Science des Matériaux (URA CNRS 155), Université Henri Poincaré-Nancy I, BP 239, 54506 Vandoeuvre les Nancy cedex, France

M. Hennion
Laboratoire Léon Brillouin, Centre d'Etudes Atomiques de Saclay, 91191 Gif-sur-Yvette cedex, France
(Received 4 March 1996)

We present a magnetization and neutron-diffraction study of the basal plane magnetic structure of Dy epitaxial films and Dy/Er superlattices. The thermal evolution of the magnetic phases, the stability of the helical phase under a magnetic field, the thermal variation of the dysprosium in-plane and c parameters, and of the dysprosium turn angle are successively shown. In Dy/Er superlattices, the dysprosium helix propagates coherently through paramagnetic erbium; at low temperature, individual dysprosium layers undergo a ferromagnetic transition and are coupled antiferromagnetically to each other for erbium layers thicknesses larger than 20 Å. In dysprosium films, as expected from the epitaxy effect, the Curie temperature of dysprosium is reduced if dysprosium is grown on yttrium and increased if it is grown on erbium, whereas it is unexpectedly close to the bulk value in Dy/Er superlattices. This amazing value of the Curie temperature in superlattices is correlated to two main experimentally observed effects: (i) the magnetoelastic driving force is reduced compared to bulk dysprosium because of the clamped γ distortion; (ii) the difference between the exchange energies in the helical and the ferromagnetic phases is increased compared to the bulk value. [S0163-1829(96)06034-1]

I. INTRODUCTION

Layered magnetic materials have generated a large interest over the several past years. Among them, epitaxial films and superlattices constituted of rare earths have shown new magnetic effects due both to the epitaxy and to the superperiodicity.

In rare-earth superlattices at least four spectacular effects have been evidenced: (i) a long-range coherence of helical magnetic phase through nonmagnetic layers, (ii) a long-range antiferromagnetic order between ferromagnetic layers through nonmagnetic ones, (iii) enhancement or reduction of the ferromagnetic transition temperature, and (iv) shift of the wave vectors in helical phases.

However, most of the rare-earth films and superlattices studied up to now were composed of magnetic layers (Gd,Dy,Er,Ho) separated by nonmagnetic ones (Y,Lu);[1–6] few works have been devoted to systems constituted of two magnetic elements such as Gd/Dy (Ref. 7) and Ho/Er.[8] As the Dy/Er system, which is the object of the present paper, they permit the study of some of the effects mentioned above and they exhibit specific behaviors due to the fact that both elements have their own magnetic characteristics.

The Dy/Er system is constituted of two magnetic elements which present opposite anisotropy: the basal plane (0001) of the hexagonal lattice is an easy magnetization plane for dysprosium, whereas the easy magnetization direction of erbium is along the c axis. In addition, both bulk materials exhibit their own succession of complex magnetic phases with temperature. Bulk dysprosium orders from the paramagnetic to the helical state at $T_N=179$ K.[9] Below this temperature, the magnetic moments are in the basal plane and the helix wave vector q_{Dy} is along the c axis. The turn angle $\omega_{\mathrm{Dy}}=2\pi/q_{\mathrm{Dy}}$ between the magnetic moments carried by atoms located in plane separated from $c/2$ decreases from 44° at T_N to 26° at $T_C=89$ K where it drops to 0°.[9] This drop corresponds to the occurrence of a ferromagnetic phase in which the moments are oriented along the a direction in the basal plane.

Erbium orders at 85 K. Below this temperature, the magnetic moments present a c-axis sinusoidally modulated structure,[10] whose wave vector is q_{Er}. The transverse moment components are disordered down to 52 K and exhibit helical ordering at lower temperature. Progressively the c-modulated structure squares up with, as shown recently,[11] a lot of lock-in and spin slip phases. At 20 K, the c-axis order becomes ferromagnetic whereas the basal component order remains helical. It results in a conical arrangement with apex angle of about 25°. The turn angle (or equivalent turn angle in the c-axis modulated structure) $\omega_{\mathrm{Er}}=2\pi/q_{\mathrm{Er}}$ is larger than the turn angle of dysprosium and varies from 51.4° to 45°.

As will be noted in Sec. V, both dysprosium and erbium lattices undergo progressive strains in the modulated phase when the temperature decreases, and discontinuous strains occur at the ferromagnetic transition.

This paper is mainly devoted to the basal plane magnetic properties of Dy/Er superlattices. Indeed, the magnetization measurements presented here have been performed with the field applied in the plane of the sample [the (0001) plane] and the response is therefore mainly due to the magnetic components in this plane. On the other hand, most of the neutron-scattering experiments shown here have been performed along the $\mathbf{c}^*$ direction around the (0002) reflection, and the component of the magnetization along the c axis does not bring any contribution to such spectra. In the samples studied, as in bulk materials, we will see that the

TABLE I. Nominal compositions of the Y/Dy/Y and Er/Dy/Er trilayers, and of the Dy/Er superlattices. The *c* parameter corresponds to the dysprosium parameter (in the trilayers) or to the average parameter (in the superlattices). They have been determined by x-ray diffraction, as well as the structural coherence length.

		Nominal composition	*c* parameter (Å)	Structural coherence length (Å)
	Tr. *A*	Y/Dy 600 Å/Y	5.630	450
	Tr. *B*	Y/Dy 2900 Å/Y	5.632	780
	Tr. *C*	Y/Dy 3200 Å/Y	5.643	760
Trilayers	Tr. *D*	Er/Dy 200 Å/Er		
	Tr. *E*	Er/Dy 450 Å/Er	5.662	400
	Tr. *F*	Er/Dy 600 Å/Er	5.666	580
	Tr. *G*	Er/Dy 3000 Å/Er	5.651	960
	Sl. *A*	Y/[Dy(34 Å)/Er(23 Å)]×50/Y	5.589	780
	Sl. *B*	Y/[Dy(60 Å)/Er(60 Å)]×60/Y	5.612	960
	Sl. *C*	Y/[Dy(35 Å)/Er(111 Å)]×47/Y	5.589	820
Superlattices	Sl. *D*	Y/[Dy(70 Å)/Er(59 Å)]×20/Y	5.603	740
	Sl. *E*	Y/[Dy(35 Å)/Er(11 Å)]×80/Y	5.621	860
	Sl. *F*	Y/[Dy(19 Å)/Er(19 Å)]×40/Y	5.600	860
	Sl. *G*	Y/[Dy(10 Å)/Er(10 Å)]×60/Y	5.605	600
	Sl. *H*	Er/[Dy(24 Å)/Er(26 Å)]×60/Er/Y	5.621	730

dysprosium moments are kept in the hexagonal basal plane and that the erbium moments have their largest component along the *c* direction. This paper is therefore rather devoted to the dysprosium magnetic behavior than to the erbium one, although both magnetic behaviors cannot be dissociated.

In order to better understand the properties of the Dy/Er superlattices where both epitaxial and superperiodicity effects are mixed, we simultaneously carried out a magnetic study of unique dysprosium films sandwiched between erbium layers: they are referred to as Er/Dy/Er trilayers. In these samples, where no superperiodicity manifests, it should be possible to focus on epitaxial effects. Moreover, Y/Dy/Y trilayers have been studied to permit comparisons between two trilayers systems where the epitaxial strains are of opposite signs, because interatomic distances in yttrium and erbium are, respectively, larger and smaller than in dysprosium.[12] In these various types of samples, we have investigated not only the usual magnetic parameters, but also the thermal dependence of the lattice parameters, which are strongly related to the magnetic phase transitions and to the mechanisms which drive these transitions.

This paper will be presented as follows. In Sec. II, we recall the elaboration technique of the samples and present their characterization by x-ray diffraction. Section III is devoted to neutron-scattering experiments conducted along the $\mathbf{c}^*$ direction around the (0002) reflection under zero magnetic field. The thermal evolution of the spectrum shows the occurrence of different magnetic phases (helical, antiferromagnetic or ferromagnetic) and of the long-range magnetic coupling between the layers. Section IV reports magnetization measurements performed with a standard superconducting quantum interference device (SQUID) magnetometer. These measurements allow ones to determine the stability of the helical phase under magnetic field. Section V is devoted to the study of the magnetoelastic effects: the α strains are investigated through the thermal variation of the *c* parameter and the γ distortion is estimated from neutron-scattering experiments along the $\mathbf{a}^*$ direction around the (1010) reflection. Section VI deals with the thermal evolution of the turn angle in the helical phase, which is related to the difference between the exchange energies in the ferromagnetic and helical phases. Finally the results are discussed in Sec. VII.

II. ELABORATION AND CHARACTERIZATION OF THE SAMPLES

MBE growth

The rare-earth samples are grown along the (0001) direction by molecular-beam epitaxy (MBE) in a chamber whose base pressure is typically in the 10^{-11} Torr range. Following the process proposed by Kwo, Hong, and Nakahara,[13] a 1000 Å thick (110) niobium buffer is first deposited on the (1120) sapphire substrate maintained at 800 °C, to prevent reaction between the rare earths and the sapphire. Then a seed layer of several hundred angstroms (yttrium or erbium) is grown during the cooling of the substrate from 800 to 400 °C. The superlattice, or the unique dysprosium layer, is subsequently deposited at 400 °C and is covered by a cap layer of the same element as the seed (yttrium or erbium). If the final layer is erbium, an yttrium layer is also deposited to inhibit oxidation of the sample when exposed to air. The rare earths are evaporated from effusion cells.

The samples (trilayers and superlattices) are gathered in Table I. Let us underline that only one superlattice (Sl. *H*) was deposited on an erbium seed layer and covered by an erbium cap layer.

X-ray diffraction

The total scattered intensity from a superlattice is given by the square of the total structure factor $|f(\mathbf{q})|^2$ which in the case of an ideal superlattice with sharp interfaces (i.e., the

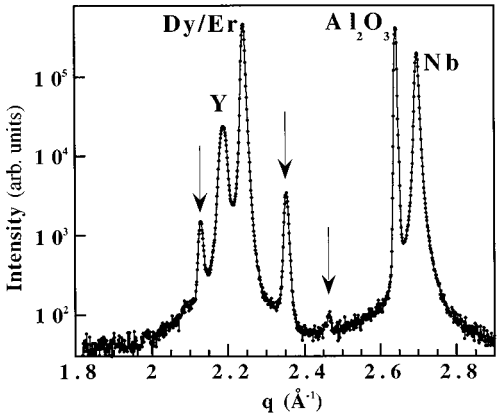

FIG. 1. Room-temperature x-ray-diffraction pattern from a [Dy (34 Å)/Er (23 Å)]×50 superlattice. The Bragg peaks of the yttrium seed and cap layers, of the niobium buffer and of the substrate are, respectively, referred to as Y, Nb, and Al_2O_3. The average (0002) Bragg peak (Dy/Er) is surrounded by satellites (indicated by arrows).

concentration and the c-parameter profiles are assumed to be rectangle-wave modulated) can be written:

$$f(q)=\frac{\sin(N\Lambda q/2)}{\sin(\Lambda q/2)}\left[f_{\mathrm{Dy}}\frac{\sin(n_{\mathrm{Dy}}qc_{\mathrm{Dy}}/2)}{\sin(qc_{\mathrm{Dy}}/2)}+\exp(i\Lambda q/2)f_{\mathrm{Er}}\frac{\sin(n_{\mathrm{Er}}qc_{\mathrm{Er}}/2)}{\sin(qc_{\mathrm{Er}}/2)}\right], \quad (1)$$

where q is the wave-vector transfer, f_{Dy} and f_{Er} are the atomic scattering amplitudes for x rays, N is the total number of bilayers, Λ is the chemical modulation of the superlattice, $n_{\mathrm{Dy(Er)}}$ is the number of dysprosium (erbium) atomic planes in an individual layer, and $c_{\mathrm{Dy(Er)}}$ is the c parameter of dysprosium (erbium).

The x-ray-diffraction pattern of the superlattice Sl. *A* (Y/[Dy(34 Å)/Er(23 Å)]×50/Y) (Fig. 1) shows the Bragg peaks of (0002) yttrium, (1120) sapphire, and (110) niobium. The average Bragg peak of (0002) dysprosium/erbium superlattice is surrounded by satellites separated by $2\pi/\Lambda$ (indicated by arrows).

The position of the (0002) dysprosium peak in the trilayers, or of the average Bragg peak in the superlattices, permits to determine the c or average c parameter (Table I). As expected from the lattice mismatch between the elements, the c parameter in the dysprosium films grown between yttrium (erbium) increases (decreases) with the dysprosium thickness. In the superlattices, the average c parameter increases with the ratio (Dy thickness)/(Er thickness). The half width at half maximum of this Bragg peak is related to the structural coherence length, which is generally around 800 Å in all the superlattices (Table I). The values corresponding to the Er/Dy 200 Å/Er trilayer are not indicated in the table, because the dysprosium Bragg peak is not intense enough to make a proper fit. Rocking curves performed on the superlattices and on the trilayers confirm a good crystal quality with mosaic widths around 0.25°.

The interface between the rare earths has not been studied in detail for the Dy/Er system. In the Er/Y system, Borchers *et al.*[14] have fitted the x-ray data to a damped rectangle-wave model, in order to obtain specific information about the structure and composition of the superlattices near the interfaces. According to these authors, the interdiffusion is quite minimal and the composition reaches 85% of the pure element within about two planes on either side of the interface. Beach *et al.*[3] and Jehan *et al.*[5] also reported that the interface between rare-earth layers prepared in the 300–400 °C temperature range is rather sharp (approximately four atomic planes). Concerning the c-spacing modulation, Borchers *et al.*[14] mentioned that the variation is also quite abrupt in Er/Y superlattices.

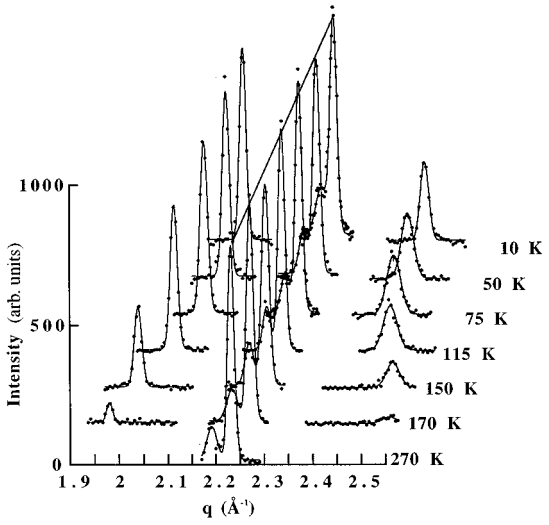

FIG. 2. Neutron-scattering spectra measured at different temperatures along the **c*** direction around the (0002) reflection for a Y/Dy (600 Å)/Y trilayer.

III. NEUTRON-SCATTERING EVIDENCE OF THE BASAL PLANE MAGNETIC PHASES

Neutron-scattering experiments were performed at the Laboratoire Léon Brillouin (CEA) in Saclay (France) on the G4.3 triple-axis spectrometer with the analyzer set for zero-energy transfer and used to minimize the background. The wavelength was 4.245 Å and the collimators were 30′ on each side of the sample and were 60′ before the detector.

Er/Dy/Er and Y/Dy/Y trilayers

A set of neutron-scattering spectra collected from sample Tr. *A* [Y/Dy (600 Å)/Y] along the **c*** direction around the (0002) reflection is shown in Fig. 2. At 270 K, the (0002) Bragg peak of yttrium is located at $q=2.191$ Å^{-1} and that of (0002) dysprosium at $q=2.232$ Å^{-1}: their relative intensity is due to the small nuclear coherent scattering amplitude of neutron in yttrium compared to that in dysprosium. When the temperature is lowered, two magnetic satellites arise symmetrically on both sides of the (0002) peak of dysprosium. These peaks located at $2\pi/\Lambda_{\mathrm{mag}}$ from the (0002) peak of dysprosium are of magnetic origin and are due to the magnetic helical modulation which develops below T_N with a wavelength Λ_{mag}. The magnetic peaks persist down to 10 K and on the whole temperature range, there is no change of the intensity of the (0002) peak of dysprosium. This clearly

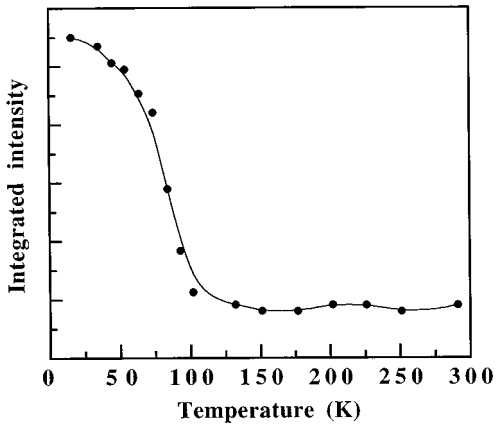

FIG. 3. Thermal variation of the integrated intensity of the Dy (0002) Bragg peak measured by neutron scattering along the **c*** direction around the (0002) reflection for a Er/Dy (600 Å)/Er trilayer.

indicates that the helical phase is stable down to the lowest temperature and that there is no ferromagnetic transition, which is dramatically different from the magnetic behavior of bulk dysprosium, where the ferromagnetic transition takes place at 89 K. The neutron-scattering results are very different in sample Tr. *F* [Er/Dy (600 Å)/Er] where a dysprosium film of identical thickness is sandwiched between erbium layers. The spectra are similar at high temperature and below the Néel temperature with the appearance of magnetic satellites, but they are very different at low temperature where the magnetic satellites disappear and the intensity of the (0002) Bragg peak of dysprosium increases. The thermal evolution of the integrated intensity of the (0002) Bragg peak of dysprosium is shown in Fig. 3. The ferromagnetic transition is indicated by the sudden increase in this intensity. The transition starts near 100 K, which is above the Curie temperature of bulk dysprosium, but it is not as abrupt as in bulk element. The increase of the Bragg peak intensity is accompanied by the disappearance of the magnetic satellites but there is a coexistence of the two phases over 20 K.

So, from neutron diffraction around the (0002) reflection, it is clear that the epitaxy of dysprosium between yttrium layers favors the helical order, whereas the epitaxy between erbium layers enhances the Curie temperature, and therefore favors the ferromagnetic phase. This is obviously consistent with the previous observations performed on dysprosium layers grown on Y_xLu_{1-x} layers whose parameters were larger or smaller than that of dysprosium, depending on the composition x.[15]

Dy/Er superlattices

The total intensity of nonpolarized neutrons scattered from a superlattice is given by

$$I(\mathbf{q})=|f_{\mathrm{nuc}}(\mathbf{q})|^2+|f^{+}_{\mathrm{mag}}(\mathbf{q})|^2+|f^{-}_{\mathrm{mag}}(\mathbf{q})|^2, \qquad (2)$$

where $f_{\mathrm{nuc}}(\mathbf{q})$ is the total nuclear structure factor and $f^{+}_{\mathrm{mag}}(\mathbf{q})$ and $f^{-}_{\mathrm{mag}}(\mathbf{q})$ are magnetic structure factors. The expression of the nuclear structure factor is quite similar to that of the x-ray structure factor given by relation (1), except that f_{Dy} and f_{Er} have to be replaced by the corresponding coherent

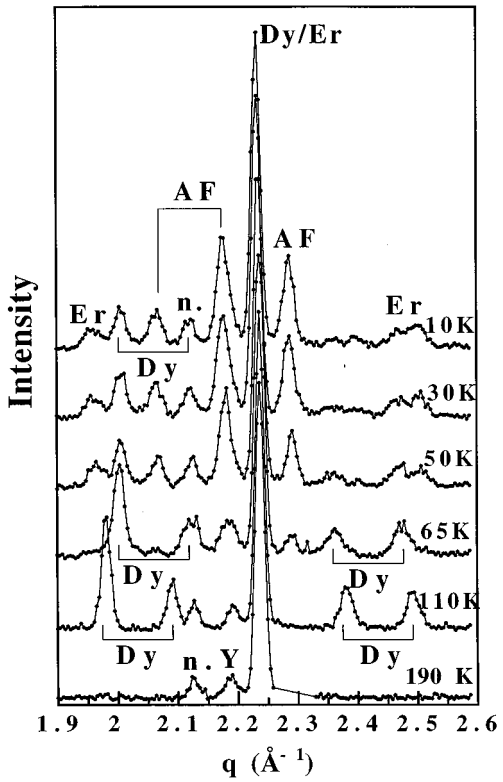

FIG. 4. Neutron-scattering spectra measured at different temperatures along the **c*** direction around the (0002) reflection for a Y/[Dy (34 Å)/Er (23 Å)]×50/Y superlattice.

neutron-scattering amplitudes b_{Dy} and b_{Er}. The expressions of the magnetic structure factors depend on the magnetic configuration; they are given in Sec. VI in the case of an helical ordering.

The set of spectra obtained by neutron-scattering experiments along the $(000l)$ direction collected from the superlattice Sl. *A* is pictured in Fig. 4. The three peaks present at 190 K correspond to the average (0002) Bragg peak of the superlattice (at a wave vector $q_0=2.237$ Å^{-1}), a satellite $(n.)$ due to the chemical modulation Λ and the Bragg peak due to the yttrium seed and cap layers (Y).

At 110 K, an additional set of peaks (Dy) of magnetic origin appear on either side of q_0, whereas the intensity of the main Bragg peak remains unchanged. The occurrence of magnetic satellites reveals the presence of the helical ordering in the dysprosium. The fact that they are split into several peaks separated by $2\pi/\Lambda$ proves that the helix propagates coherently through paramagnetic erbium layers. The fit of the spectra and the thermal evolution of the turn angle between moments in dysprosium layers and of the effective turn angle in erbium will be discussed in Sec. VI. The propagation of the helix through a spacer was originally shown in systems where the spacer between magnetic layers is nonmagnetic, Dy/Y,[16] Er/Y,[4] Ho/Y,[5] Dy/Lu,[3] Ho/Lu.[6] It is now observed when the spacer is paramagnetic, Dy/Er,[17] Ho/Er.[8] This phenomenon is due to the stabilization of a spin-density wave in the conduction band of erbium, which then couples to the local moments on the dysprosium sites.[2]

With decreasing temperature the magnetic peaks positions move in towards q_0 because of the increase of the wavelength of the magnetic modulation Λ_{mag}. From the width of

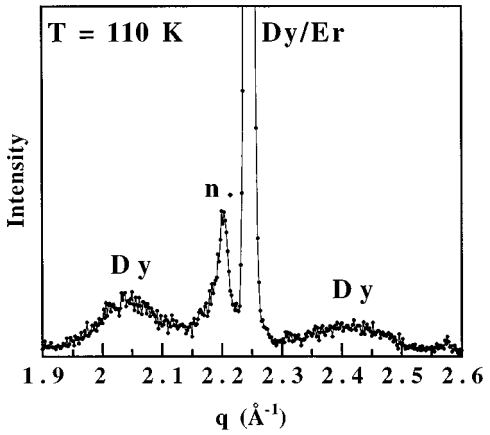

FIG. 5. Neutron-scattering spectrum measured at 110 K along the **c*** direction around the (0002) reflection for a Y/[Dy (35 Å)/Er (111 Å)]×47/Y superlattice.

these magnetic peaks, one can deduce that the magnetic coherence length decreases with the temperature: it varies from 550 Å at 110 K to 450 Å at 80 K. On the other hand, as already observed in other systems, the magnetic coherence length of the helical phase of dysprosium is a function of the thickness of the spacer. For an erbium spacer thickness of 111 Å (Sl. *C*), the width of the central magnetic satellites encompasses the bilayers harmonic position rendering them unresolved (Fig. 5) and the basal plane magnetic coherence at 110 K is limited to one dysprosium layer. This result has to be compared with the loss of coherence observed in a Dy/Lu superlattice for a 80 Å lutetium thickness[3] and in a Dy/Y superlattice for a 120 Å yttrium thickness.[18]

Below 50 K new peaks emerge (referred to as AF in Fig. 4) at positions corresponding to a modulation twice of the chemical modulation. These peaks are the sign of an antiparallel arrangement between dysprosium ferromagnetic layers. The coherence length of this antiferromagnetic phase is 400 Å at 60 K and 300 Å at 10 K. A transition from an helical phase inside the layers, coherent through the spacer, to a ferromagnetic order inside each layer with antiparallel coupling between the magnetic layers through the spacer has been observed previously in the Dy/Lu system,[3] where lutetium is nonmagnetic. However, the situation is different in the Dy/Er system, because erbium is a spacer which presents an ordered complex magnetic phase in this temperature range. Note that, despite the occurrence of this antiparallel arrangement, the satellites attributed to the magnetic helix do not totally disappear and persist until 10 K; at this temperature the magnetic coherence length of the residual helical order is about 300 Å. In addition to the (AF) peaks, new peaks located at 1.972 and 2.518 $Å^{-1}$ (Er) take place below 50 K. They are due to the helical ordering of the erbium basal plane component.

Thus at low temperature, the configuration of dysprosium is an antiferromagnetic stacking of the ferromagnetic dysprosium blocks, with a residual helical phase whose persistence remains to be explained. The magnetic configuration of erbium presents an helical in-plane component. Similar succession of the magnetic phases has been observed in the superlattices Sl. *B* and Sl. *F*.

The coexistence of the two magnetic configurations in the

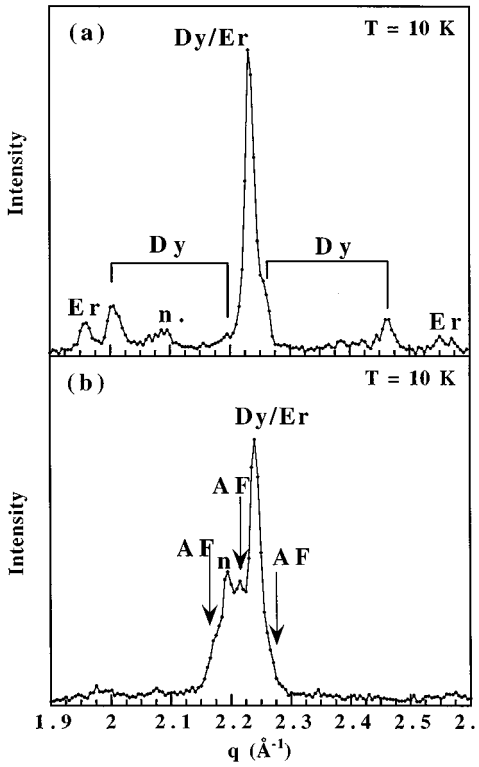

FIG. 6. (a) Neutron-scattering spectrum measured at $T=10$ K along the **c*** direction around the (0002) reflection for a Er/[Dy (24 Å)/Er (26 Å)]×60/Er superlattice. (b) Neutron-scattering spectrum measured at $T=10$ K along the **c*** direction around the (0002) reflection for a Y/[Dy (70 Å)/Er (59 Å)]×20/Y superlattice.

dysprosium layers at low temperature can be the result of a thermodynamic equilibrium, or it can be due to fan structures or inhomogeneities in the sample. As a seed layer of yttrium was present in most of the samples, we could think that the part of the sample close to yttrium was not submitted to the same strain as the part of the sample located in the middle of the superlattice. For that reason, we prepared the sample Sl. *H* with erbium as a seed layer and as a cap layer. As shown in Fig. 6(a), the helical phase is still present at low temperature. The buffer probably plays a role on the strains in the sample but it does not seem to induce the coexistence of the phases. In fact, we observed a correlation between the thickness of the individual dysprosium layers and the relative importance of the helical phase at 10 K: the thicker the dysprosium layers are, less residual helical component is present. For example there is practically no residual helix at 10 K in sample *D* where dysprosium layers are 70 Å thick, although the superlattice has been grown between 500 Å thick yttrium layers [Fig. 6(b)]. This observation could lead to invoke an effect occurring at the interfaces, but the long-range character of this residual phase is incompatible with such an explanation.

In all the samples studied before, the intensity of the average (0002) Bragg peak is temperature independent, which means that there is no ferromagnetic long-range order. As shown in a previous paper devoted to the sample Sl. *B*,[19] the antiparallel arrangement between dysprosium layers and the residual helical component are both destroyed by applying a magnetic field in the plane of the sample, and they are re-

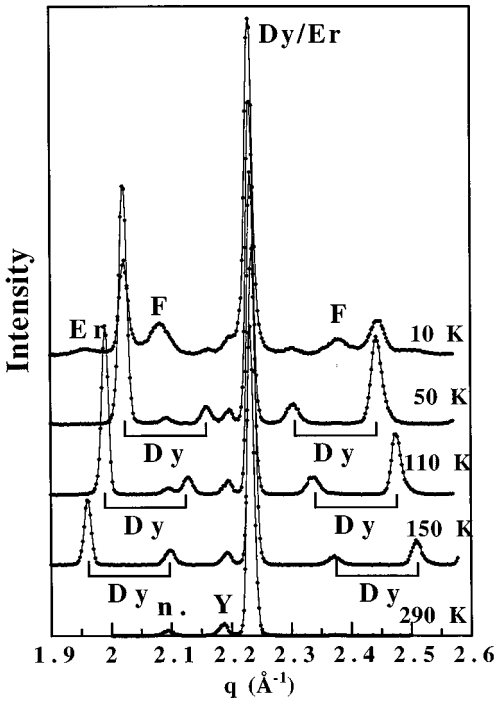

FIG. 7. Neutron-scattering spectra measured at different temperatures along the **c*** direction around the (0002) reflection for a Y/[Dy (35 Å)/Er (11 Å)]×60/Y superlattice.

placed by a long-range ferromagnetic phase. Moreover, this transformation is irreversible: when suppressing the field, the system remains actually ferromagnetic. Neither the antiferromagnetic peak nor the residual helix contribution reappear. It is necessary to warm up the sample at about 80 K and to cool it down under zero magnetic field to recover the antiparallel stacking.

Let us finally mention the behavior of sample Sl. *E* (Fig. 7) where the thicknesses of erbium and dysprosium layers are small.[20] At room temperature, the neutron-scattering pattern exhibits, as in Fig. 4, the average (0002) peak, the yttrium buffer contribution (Y) and a nuclear satellite ($n.$). When decreasing the temperature, split helical satellites, corresponding to the occurrence of the helical phase of dysprosium with coherence through erbium, appear on each side of the average Bragg peak. Their intensity is the largest at 50 K and decreases below this temperature. However, contrarily to the previous samples, their intensity is not transferred to antiferromagnetic peaks but to two peaks referred to as *F* (Fig. 7) separated from the (0002) peak by $2\pi/\Lambda$, and which are therefore of ferromagnetic origin. Because they are however broad and slightly shifted compared to the peak referred to as $n.$, the coherence length of the ferromagnetic order is rather small (150 Å). This ferromagnetic contribution also appears on the (0002) peak: its intensity increases and a broad contribution takes place in the foot of this peak. The application of a magnetic field of 3 kOe leads to the suppression of the helical phase and to the increase of the ferromagnetic contribution in the main peak and in the satellites. The coherence length of the ferromagnetic phase is then 380 Å and persists if the field is suppressed.

Thus at low temperature, the magnetic order in the dysprosium layers is ferromagnetic, with a residual helical phase

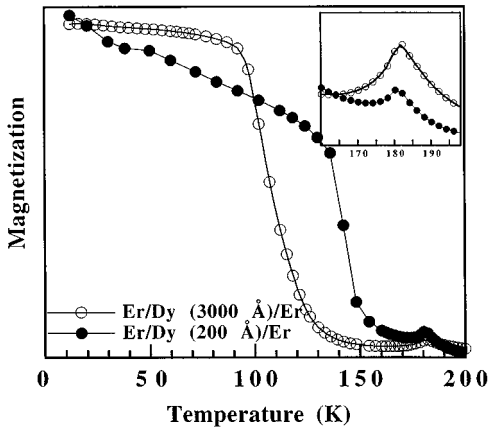

FIG. 8. Thermal variation of the magnetization for the Er/Dy (3000 Å)/Er and Er/Dy (200 Å)/Er trilayers under a 2.6 kOe magnetic field applied in the plane of the sample.

whose contribution decreases in the case of thick dysprosium layers. The ferromagnetic dysprosium layers constitute an antiparallel stacking through the erbium layers in most of the samples, and a parallel one when the erbium thickness is small. Such a ferromagnetic arrangement between successive magnetic layers when the spacer thickness is small has already been observed in the Dy/Lu system.[3]

IV. MAGNETIZATION MEASUREMENTS

In order to study the stability of the helical phase, magnetic measurements have been performed using a standard SQUID magnetometer. As mentioned in the Introduction, the magnetic field was applied in the basal plane, which means that we explored mainly the magnetism in the dysprosium layers. The 0–70 kOe field range was systematically explored.

Néel temperature of dysprosium

Cooling the sample under a magnetic field allowed us to determine the Néel temperature of dysprosium. Figure 8 presents the curves obtained for two Er/Dy/Er trilayers (Tr. *D* and Tr. *G*), where the dysprosium thicknesses, respectively, are 200 and 3000 Å. As shown in the inset, the magnetic ordering leads to an increase of the susceptibility, and therefore to a cusp, indicating the Néel temperature. The Néel temperatures measured for Er/Dy/Er trilayers and Dy/Er superlattices are given in Fig. 9 versus the dysprosium thickness. The thicknesses above 100 Å correspond to the Er/Dy/Er trilayers, whereas the thicknesses below correspond to the Dy/Er superlattices. In the trilayers, T_N decreases from 182 K in Er/Dy (3000 Å)/Er to 180 K in Er/Dy (110 Å)/Er. In the superlattices, where the thickness of the individual dysprosium layers is smaller, T_N decreases from 176 K in the [Dy (70 Å)/Er (59 Å)]×20 superlattice to 147 K in the [Dy (10 Å)/Er (10 Å)]×20 superlattice. As the same trend has also been observed in Y/Dy/Y trilayers where the epitaxial strains are of opposite sign, the thickness of the dysprosium layer seems to be the main parameter leading to a change of the Néel temperature.

This could be due to the fact that, the thinner the layers are, the more important is the number of atoms which are

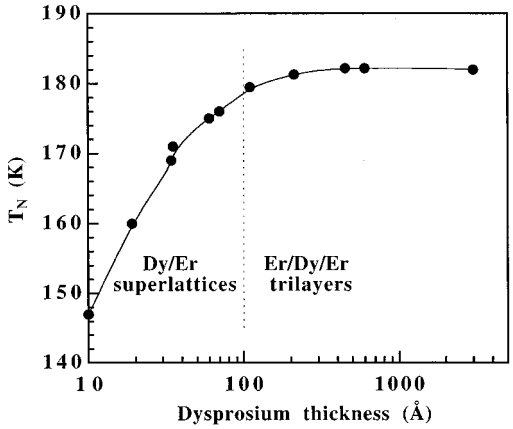

FIG. 9. Variation of the Néel temperature T_N versus the dysprosium thickness (in a logarithmic scale) in Er/Dy/Er trilayers and Dy/Er superlattices.

proportionally involved in the interfaces and which have therefore less neighbors than the atoms in the middle of the layer. An effect of alloying at the interface, which is of course relatively more important as the thickness is smaller, may also be responsible for such a trend, because the Néel temperature of bulk Dy_xEr_{1-x} alloy decreases with x.

Let us finally underline that the increase of the magnetization observed in Fig. 8 occurs at different temperatures in the two trilayers, the thinner dysprosium film exhibiting a higher Curie temperature than the 3000 Å thick dysprosium film. This crucial phenomenon is exposed and discussed in some detail in the following paragraph.

Magnetization in the trilayers

The first magnetization curves collected from the Er/Dy (600 Å)/Er and Y/Dy (600 Å)/Y trilayers at different temperatures are pictured in Figs. 10 and 11, respectively. All theses curves have been obtained after zero-field cooling from a temperature higher than the Néel temperature. The magnetization is given in μ_B per atom of dysprosium.

Let us first consider the evolution of the magnetization of the sample Er/Dy (600 Å)/Er (Fig. 10). At 180 K (just above

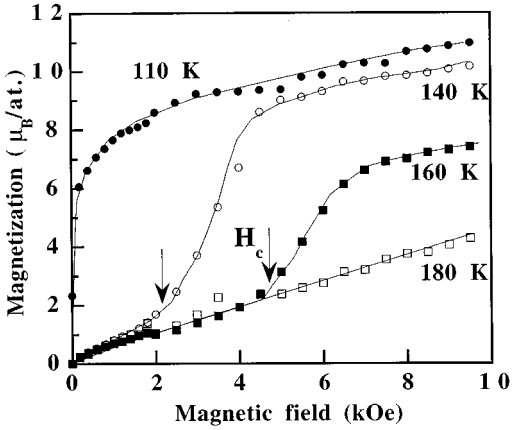

FIG. 10. First magnetization curves measured at different temperatures for the Er/Dy (600 Å)/Er trilayer.

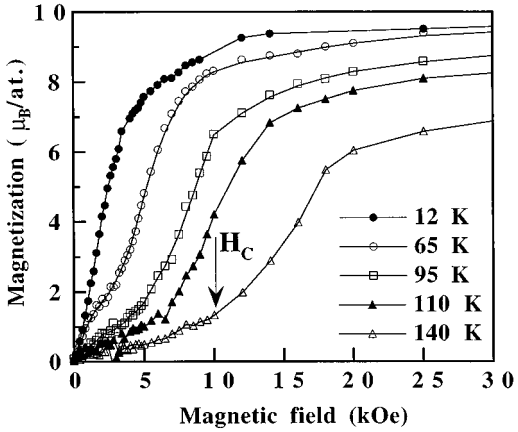

FIG. 11. First magnetization curves measured at different temperatures for the Y/Dy (600 Å)/Y trilayer.

the Néel temperature), the magnetization increases linearly with the field in the whole field range we explored. At 160 K, the magnetization exhibits first a domain of low susceptibility corresponding to the stability of the helical phase. At a critical field H_C, the increase of the magnetization reveals the onset of the ferromagnetic transition. The same phenomenon is observed at 140 K with a lower critical field. At 110 K, the susceptibility is very large at zero field, which means that dysprosium is in the ferromagnetic state.

These curves have to be compared to the classical curve of the magnetization measured in bulk dysprosium single crystals.[21] If the general trends are the same, a number of differences are to be underlined: (i) the critical field which drives the ferromagnetic transition at a given temperature is smaller in the Er/Dy/Er trilayer than in bulk dysprosium (in bulk dysprosium, H_C is 10 kOe at 160 K, 7 kOe at 140 K, and 3 kOe at 110 K); this is consistent with neutron-scattering experiments showing that the ferromagnetic phase of dysprosium is stabilized in the dysprosium films grown on erbium; (ii) the ferromagnetic transition is smoother in the trilayer than in bulk dysprosium. Indeed in bulk dysprosium, the transition spreads on about $\Delta H_C \approx 0.3$ kOe at 160 K and $\Delta H_C \approx 0.1$ kOe at 140 K, whereas it is as large as 2 kOe in the trilayer for the same temperatures. It means there is certainly a domain of field and temperature in which the ferromagnetic and helical phases coexist.

Figure 11 confirms that the helical phase is stabilized in Y/Dy/Y trilayers. Compared to Fig. 10, the fields referred as H_C are shifted to the high values (the magnetic field scale is multiplied by three) and there is no temperature below which the susceptibility is very high in zero field. It is to underline that below 65 K, the low susceptibility domain is very reduced and it is difficult to determine H_C. However, as shown in the neutron-scattering pattern (Fig. 2), there is absolutely no ferromagnetic component at 10 K. On the other hand, as in Fig. 10, the transitions towards the ferromagnetic state are very smooth: at 140 K, ΔH_C reaches 10 kOe.

The critical fields H_C determined from the first magnetization curves are gathered in Fig. 12 for several Y/Dy/Y and Er/Dy/Er trilayers. The temperatures where this critical field drops to 0 can be considered as the Curie temperatures. Compared to the bulk behavior, there is clearly a stabilization of the ferromagnetic phase in the Er/Dy/Er trilayers and,

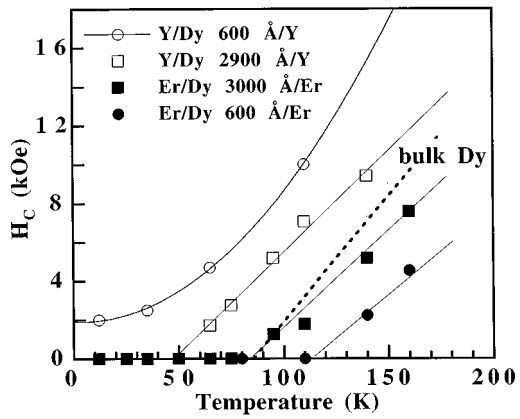

FIG. 12. Thermal variation of the critical field H_C necessary to drive the ferromagnetic transition in Y/Dy/Y and Er/Dy/Er trilayers. The dotted line represents the variation for bulk Dy.

at the opposite, a stabilization of the helical phase in the Y/Dy/Y trilayers. The critical field measured in the Y/Dy 600 Å/Y trilayer never drops to 0, because the ferromagnetic transition under 0 magnetic field is suppressed, as shown previously in Sec. III (Fig. 2).

Magnetization in the superlattices

The first magnetization curves of the sample Sl. *B* ([Dy(60 Å)/Er(60 Å)]×60) are shown in Figs. 13(a) (temperature range above 65 K) and 13(b) (temperature range below 65 K). The magnetization is given in μ_B per atom, in taking account of the total number of atoms (dysprosium and erbium). Let us first underline that the measurements have been performed in the 0–70 kOe field range and that, even at 70 kOe, the magnetization never exceeds $5\mu_B$/at. This means that the magnetic component of erbium does not contribute significantly to the signal, because it is mainly oriented along the *c* axis, as in bulk erbium, and does not collapse in the (0001) plane.

Above 65 K, the general trend is the same as in the former cases. At 160 K, H_C is about 5.5 kOe, which is approximately 5 kOe below the critical field in bulk dysprosium and leads to think that, as in the Er/Dy/Er trilayers, the ferromagnetic phase is stabilized. Above this critical field, the magnetization increases more rapidly and again the transition is very broad (ΔH_C is about 4 kOe). This smooth transition could be due to a strain modulation in the dysprosium layers, especially at the interfaces with erbium. Down to 110 K, it is still possible to determine H_C, which is close to 3 kOe, that is not too far from the bulk value; the difference between the critical fields in the superlattice and in bulk dysprosium is reduced when the temperature is lowered. If we compare the magnetization curves measured at 110 K for the Er/Dy 600 Å/Er trilayer (Fig. 10) and for the superlattice Sl. *B* [Fig. 13(a)], it is obvious that, at a given temperature, the ferromagnetic phase is less stabilized in the superlattice than in the Er/Dy/Er trilayer. The critical fields are gathered for Dy/Er superlattices and for the Er/Dy 600 Å/Er trilayer in Fig. 14. The Curie temperature (that is the temperature where the critical field drops to zero) in the superlattices is clearly smaller than in the trilayer, and even smaller than the bulk

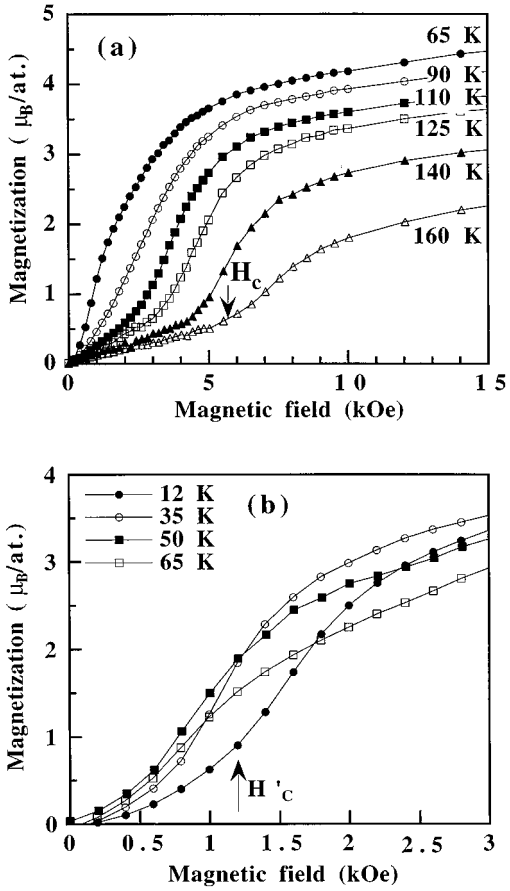

FIG. 13. (a) First magnetization curves measured at high temperatures for a Y/[Dy (60 Å)/Er (60 Å)]×60/Y superlattice. (b) First magnetization curves measured at low temperatures for a Y/[Dy (60 Å)/Er (60 Å)]×60/Y superlattice.

value. The epitaxial strains in dysprosium which should be similar and anyway of the same sign in the Er/Dy/Er trilayers and in the Dy/Er superlattices are certainly not the only reason for the shift of the Curie temperature. The specific structure of the superlattices (the superperiodicity and the thin

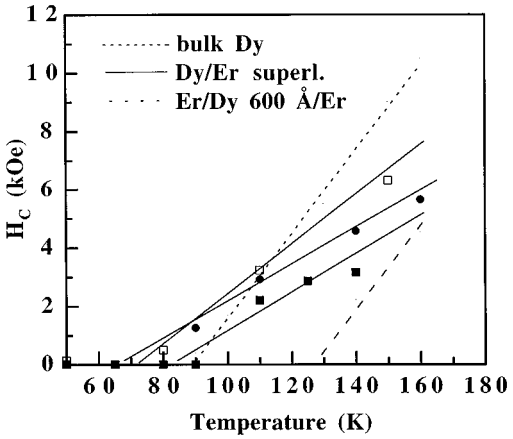

FIG. 14. Thermal variation of the critical field H_C necessary to drive the ferromagnetic transition in Dy/Er superlattices (continuous lines), in a Er/Dy/Er trilayer and in bulk Dy (dotted lines).

layers) has to be taken into account. Let us also underline that, although the dysprosium Curie temperature in the superlattices is smaller than in bulk element, the magnetic field necessary to destroy the helical phase above 110 K is higher in the bulk than in the superlattices. The coherent helical order through paramagnetic erbium is therefore not as stable as in the bulk, certainly because the dysprosium moments at the interfaces with erbium are more influenced by the applied magnetic field.

Figure 13(b) shows that the slope of the magnetization curves at the origin decreases again below 50 K and a domain of low susceptibility reappears. This is attributed to the occurrence of the antiferromagnetic coupling, observed in the neutron-diffraction spectra, which reduced the initial susceptibility. The field referred to as H_C' is the field necessary to break the antiferromagnetic long-range order. This value is consistent with the field for which the AF peaks disappear and the intensity of the main (0002) Bragg peak increases under magnetic field in the neutron-scattering spectra.[19]

V. MAGNETOELASTIC EFFECTS

Magnetoelastic modes in bulk dysprosium and erbium

The ferromagnetic transition in heavy rare earths is known to be driven by magnetostrictive effects. It occurs when the gain in magnetoelastic energy is sufficient to overcome the difference between the exchange energies in the modulated and in the aligned phases.[22] Because of the large magnetoelasticity, the succession of the different magnetic phases is accompanied by anomalous variations of the lattice parameters. In the paramagnetic phase, the parameters of dysprosium decrease with the temperature as expected from the usual thermal expansion. In the helical phase of bulk dysprosium, from T_N=179 K to T_C=89 K, the a and b in-plane parameters decrease simultaneously with temperature whereas the c parameter increases.[23] These strains correspond to an homogeneous dilatation (called α_1) combined with a cylindrical strain (called α_2). They are partially compatible with the development of the helimagnetic order along the c axis. At the ferromagnetic transition, the lattice parameters present discontinuous steps. The abrupt increase of c is due to a sudden change of the α strain modes which were already present in the helical phase but which are larger in the ferromagnetic one.[24] The opposite steps of the a and b in-plane parameters reveal an orthorhombic distortion (called γ). This γ mode is incompatible with the helical ordering and for that reason it has been said to be clamped in the helical phase. To avoid confusion with the epitaxial clamping described below, we refer to this clamping of the γ strain in the helical phase as me clamping (magnetoelastic clamping). For the same reason, the α modes are said to be submitted to a partial me clamping in the helical phase. The γ distortion is considered as the main driving force to the first-order ferromagnetic transition of dysprosium. The contribution of the α modes which can develop partly in the helical phase is considered as less important. Nevertheless, it is the occurrence of the two spontaneous strains which leads to the ferromagnetic transition.

In bulk erbium, the γ mode is totally me clamped down to the lowest temperature because an helical component is kept in the ferromagnetic phase which is in fact conical. The α mode is partially me-clamped in the c-modulated phases down to 20 K. Because the turn angle is large, the partial α mode is reduced and the increase of c and the decrease of a and b are small between 85 and 20 K. At the ferromagnetic transition the α mode becomes larger, which leads to a step in c parameter and consequently to drop a of a and b parameters.[25]

Effects of epitaxy on the magnetoelastic energy

When the basal plane of a rare earth is epitaxially grown on the basal plane of another rare earth, the two lattices are mechanically clamped to each other. We will refer to this effect as epitaxial clamping: e-clamping. As a consequence, a strain occurring in one of the rare earths induces a strain in the second one and therefore produces an increase of the elastic energy in both elements. For that reason, the γ distortion of ferromagnetic dysprosium is less favorable in a layer of dysprosium grown on another rare earth than in bulk dysprosium: such a distortion lowers the magnetostrictive energy in magnetic dysprosium but increases the elastic energy in both rare earths. It is to be stressed that, because of the sixfold symmetry of both rare earths in the basal plane, no γ strain is induced by the epitaxy itself.

Concerning the α modes, an e-clamping effect similar to that described above and unfavorable to the ferromagnetic transition is also expected. However, at the difference of the γ mode, α strains are induced by epitaxy and this effect has to be added to the e-clamping effect. Indeed, as it has been shown in the former parts of this paper, the Curie temperature of dysprosium grown on another rare earth depends on the sign of α strains induced in dysprosium by epitaxy: (i) if the epitaxial α strains induced in dysprosium represent a positive magnetostrictive energy, the helical phase is stabilized. This occurs in the Dy/Y system[26] where the parameters of bulk yttrium are larger than the parameters of bulk dysprosium; (ii) if the epitaxial α strains represent a negative magnetostrictive energy, the ferromagnetic phase is stabilized. This happens in the Dy/Lu system[3] and in the dysprosium films grown between erbium layers[12] where the parameters of lutetium and erbium are smaller than that of dysprosium.

In fact the roles of the various strain modes have not been studied in detail up to now and, in most of the papers devoted to the magnetic transition in superlattices, the α and γ modes are not clearly separated. One of the reasons is probably the lack of accurate measurements of the lattice parameters in thin films and superlattices.

α strains in Y/Dy/Y and Er/Dy/Er trilayers and Dy/Er superlattices

In the neutron-scattering spectra collected from Y/Dy/Y or Er/Dy/Er trilayers, the (0002) Bragg peaks of dysprosium, erbium, or yttrium are well separated; the position of the (0002) Bragg peak of dysprosium measured with decreasing temperature has permitted to determine the thermal evolution of the dysprosium c parameter. In the superlattices, the (0002) peak is an average peak whose position $\overline{q}$ is related to the c parameters of dysprosium and erbium c_{Dy} and c_{Er} by the relation

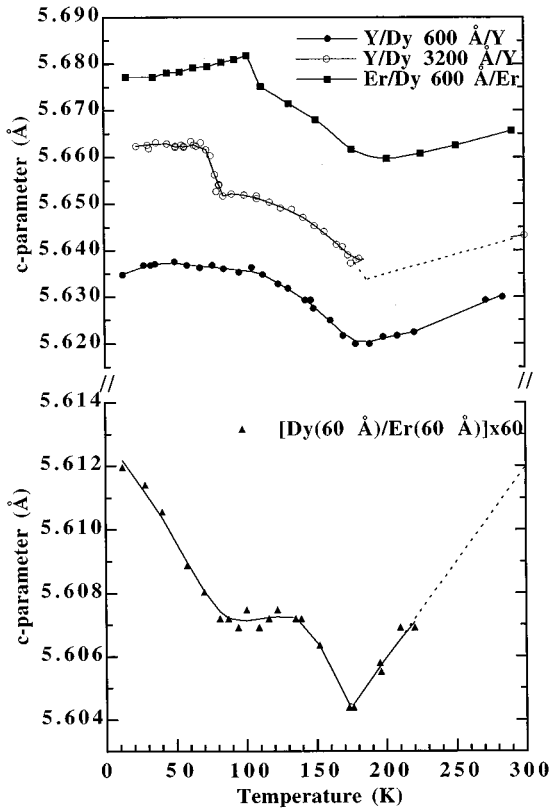

FIG. 15. Thermal variation of the c-axis parameter for Y/Dy (600 Å)/Y, Y/Dy (3200 Å)/Y, Er/Dy (600 Å)/Er trilayers, and for a Y/[Dy (60 Å)/Er (60 Å)]×60/Y superlattice.

$$\overline{q} = \frac{2\pi(n_{\mathrm{Dy}} + n_{\mathrm{Er}})}{(n_{\mathrm{Dy}} c_{\mathrm{Dy}} + n_{\mathrm{Er}} c_{\mathrm{Er}})},$$

where n_{Dy} and n_{Er} are the numbers of atomic planes in the dysprosium and erbium individual layers. The average c parameter reflects the thermal dependence of both dysprosium and erbium parameters.

Figure 15 presents the thermal evolution of c parameters obtained for the superlattice [Dy(60 Å)/Er(60 Å)]×60 as well as for Er/Dy/Er and Y/Dy/Y trilayers. Let us first discuss the values of the c parameter of dysprosium measured at room temperature in the trilayers, and compare them to the average c parameter in the superlattice. In Y/Dy/Y trilayers, dysprosium is grown between two layers of an element whose bulk parameters are larger. In the Y/Dy (3200 Å)/Y trilayer, where the dysprosium layer is thick, c_{Dy} is close to the bulk value (5.65 Å). In the Y/Dy (600 Å)/Y trilayer, where the dysprosium layer is thinner, the c_{Dy} lattice parameter is reduced. This is due to the epitaxy which tends to match the in-plane parameters of dysprosium and yttrium and, as a consequence, to expand the in-plane parameter of dysprosium and simultaneously to reduce the in-plane parameter of yttrium. Due to the elasticity of the materials, the expansion of dysprosium in the basal plane is accompanied by a reduction of the c_{Dy} parameter. In the Er/Dy (600 Å)/Er trilayer, where dysprosium is grown on an element whose bulk parameters are smaller, the effect is reversed: the in-plane parameter of dysprosium is reduced and c_{Dy} is enhanced. The difference between c parameters of dysprosium and erbium in the trilayer is then larger than the mismatch between bulk elements. This is confirmed by the difference between the positions of the (0002) Bragg peaks of dysprosium and erbium in the Er/Dy (600 Å)/Er trilayer. The peaks are separated by 0.035 $\mathrm{Å}^{-1}$ instead of 0.025 $\mathrm{Å}^{-1}$ expected from the bulk values.

In the superlattice, the measured c parameter is lower than that of dysprosium, because it is the average of the c parameter of dysprosium and the c parameter of erbium. Nevertheless, it is likely that the c parameter in the dysprosium layers is larger than in bulk dysprosium and that the c parameter in the erbium layers is smaller than in bulk erbium.

Let us discuss now the thermal dependence of the c parameter. Between room temperature and the Néel temperature T_N (approximately 179 K), the c parameter in all the samples decreases continuously with temperature because of the classical thermal contraction.

Then the helical ordering which develops below T_N in the dysprosium layers is accompanied in the trilayers by an increase of the c_{Dy} parameter when the temperature decreases. This is due to the α strains, whose contribution is related to the turn angle between magnetic moments in the helical phase.[22] This spontaneous strain adds to the epitaxial α strains, already observed at room temperature. Because this effect does not take place in erbium which is paramagnetic above 85 K, the increase of the average c parameter is reduced in the superlattice (note the change in the y scale).

At lower temperature, a discontinuous step is observed in the Y/Dy (3200 Å)/Y sample. It corresponds to the ferromagnetic transition, which takes place at a temperature close to the Curie temperature of the bulk element. Such a discontinuous step also occurs in the Er/Dy (600 Å)/Er trilayer but at a higher temperature, which is consistent with the enhancement of the Curie temperature already reported for this sample in Secs. III and IV. In the Y/Dy (600 Å)/Y trilayer, no step is observed and the lattice parameter varies continuously from T_N to 10 K, which is consistent with the stabilization of the helical phase.

In the [Dy(60 Å)/Er(60 Å)]×60 superlattice, there is no real discontinuous step as in the trilayers but when the temperature is decreased, the average c parameter in the superlattice increases sharply from a temperature close to the Curie temperature determined from the thermal dependence of the critical field (Fig. 14) and goes on increasing down to the lowest temperature.

γ distortion in Er/Dy/Er trilayers and Dy/Er superlattices: neutron diffraction along a*

In order to investigate the in-plane parameters, that is especially the γ distortion, neutron-scattering experiments were performed with the wave vector along the **a*** direction around the (1010) reflection. The patterns collected from the Er/Dy (600 Å)/Er trilayer and from the [Dy(60 Å)/Er(60 Å)]×60 superlattice are pictured in Figs. 16(a) and 16(b). At room temperature, the superlattice and the trilayer spectra exhibit an unique peak, whose widths at half maximum, respectively, are 0.0130 and 0.0137 $\mathrm{Å}^{-1}$ for a calculated resolution of 0.008 $\mathrm{Å}^{-1}$. These widths are clearly smaller than the difference between the positions of the (1010) peaks of bulk dysprosium and bulk erbium which is

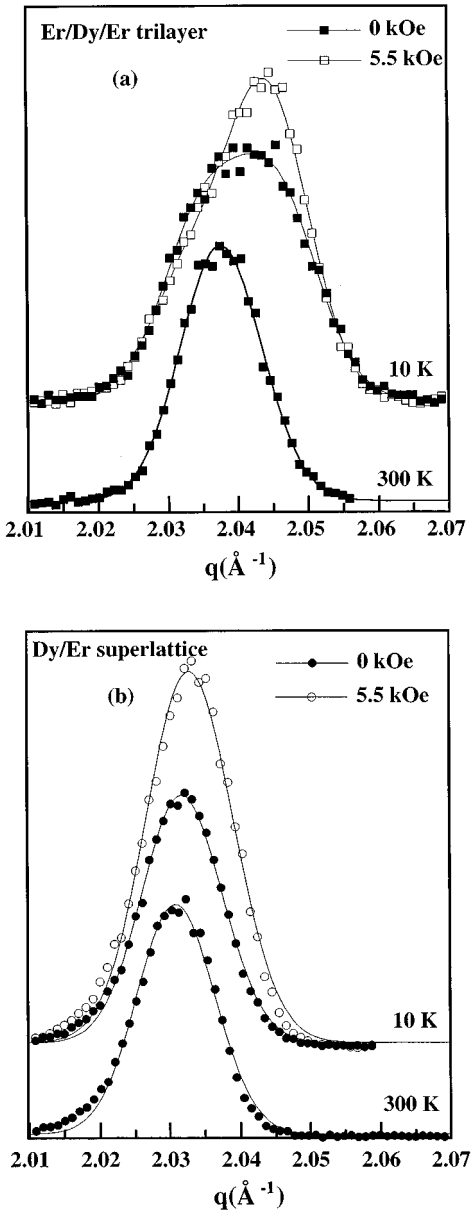

FIG. 16. (a) Neutron-scattering spectra measured along the **a*** direction around the (1010) reflection for a Er/Dy (600 Å)/Er trilayer, at 300 K under zero magnetic field, and at 10 K under 0 Oe and 5.5 kOe magnetic field. (b) Neutron-scattering spectra measured along the **a*** direction around the (1010) reflection for an Y/[Dy (60 Å)/Er (60 Å)]×60/Y superlattice, at 300 K under zero magnetic field, and at 10 K under 0 Oe and 5.5 kOe magnetic field.

about 0.02 $Å^{-1}$. If the in-plane parameters were different in both elements, we could expect two peaks (one for erbium and another one for dysprosium) with intensities in a ratio close to that observed between the intensities of the (0002) peaks of dysprosium and erbium along the **c*** direction. This unique peak shows that the in-plane parameters of the rare earths are the same in both erbium and dysprosium, or that they are very close if we consider the difference between the experimental resolution and the theoretical one. This is in agreement with the epitaxial match of the lattices. The effect is particularly spectacular in the trilayer where the layers are several hundreds angstroms thick.

When the temperature decreases, the position of the average Bragg peak in the superlattice changes very little, except it very slightly moves towards the high q values, which is consistent with the small thermal dependence of a and b parameters in bulk dysprosium above T_N, and between T_N and T_C. The main difference between the spectra obtained from the trilayer and from the superlattice is observed at lower temperature, where the width of the Er/Dy (600 Å)/Er (1010) peak increases significantly (when the temperature decreases below 110 K), whereas the width of the peak obtained from the superlattice is unchanged. The apparent increase of the width of the peak in the trilayer is interpreted by the occurrence of γ distortion in domains along the three equivalent a directions of the basal hexagonal plane.[12] The large peak would be the superposition of three peaks slightly shifted. The fact that we do not observe such broadening in the superlattice leads to the conclusion that there is no (or very few) γ distortion in this sample.

The application of a magnetic field along a direction perpendicular to the scattering vector supports this interpretation: in the trilayer, the magnetic field favors the domains along the field direction and the overall peak becomes thinner. In the superlattice, the effect is essentially to increase the intensity of the peak, which is due to the fact that the antiferromagnetic arrangement is replaced by a long-range ferromagnetic order. The peak measured under magnetic field is also very slightly shifted towards higher q values, but this corresponds to a -0.05% contraction of the b parameter, whereas this contraction is of -0.5% at the ferromagnetic transition in bulk dysprosium.

However, if the γ mode occurs in the trilayer, it is necessary to note that this γ strain does not take place abruptly at the ferromagnetic transition. Indeed, the width of the (1010) peak increases continuously from T_C down to 10 K which means that the γ distortion occurs progressively. This could be due to the e-clamping effect. These measurements lead therefore to the conclusion that the γ mode brings a reduced contribution to the driving force to the ferromagnetic transition in the trilayer and no contribution in the superlattice.

Note finally that, under zero magnetic field, the intensity of the (1010) peak does not increase at low temperature, as could be expected from a ferromagnetic transition of erbium with a net component along the c direction. It means that erbium does not undergo the ferromagnetic transition towards the conical phase. This is consistent with the fact that erbium is grown on an element with larger lattice parameters, and therefore is submitted to epitaxial strains which favor a modulated magnetic structure, as in the case of the Er/Y system.[4]

VI. EXCHANGE ENERGY: THERMAL EVOLUTION OF THE DYSPROSIUM TURN ANGLE

The turn angle ω between the dysprosium moments of consecutive (0001) planes in the modulated phase is related to the difference ΔE_{ex} between the exchange energies in the helical and in the ferromagnetic phases through the relation:

$$\Delta E_{\mathrm{ex}} \approx \sigma^2 \frac{(1-\cos\omega)^2}{\cos\omega} \frac{\cos\omega_i}{(1-\cos\omega_i)^2}, \qquad (3)$$

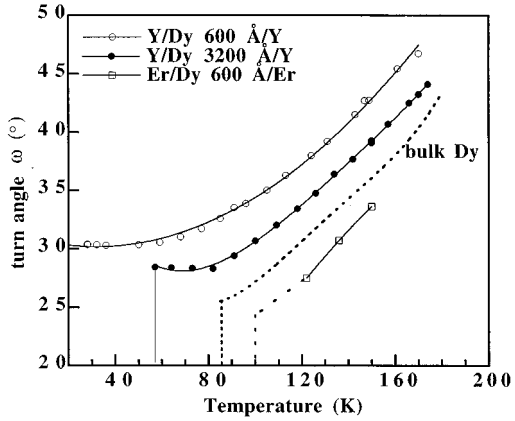

FIG. 17. Thermal variation of the turn angle between Dy moments in Y/Dy/Y and Er/Dy/Er trilayers. The dotted line represents the variation in bulk Dy.

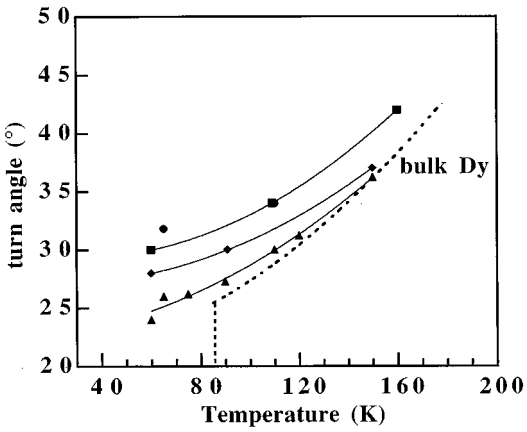

FIG. 18. Thermal variation of the turn angle between Dy moments in Dy/Er superlattices (continuous lines) and in bulk Dy (dotted line).

where σ is the reduced magnetization, ω is the turn angle, and ω_i is the initial turn angle at the ordering temperature T_N.

The turn angle of dysprosium in the trilayers is easy to determine from the well defined and nonsplitted satellites located on each side of the (0002) Bragg peak of dysprosium. The values determined for different trilayers are reported in Fig. 17 as well as the values for bulk dysprosium.

In the bulk element, the turn angle is $\omega_i = 44°$ at T_N and it decreases down to 26° at the ferromagnetic transition. Such a decrease of the turn angle of dysprosium with the temperature is also observed in all the films, but it drops to 0° at a different Curie temperature. The turn angle determined in the Y/Dy 600 Å/Y trilayer never drops to 0°, because the ferromagnetic transition is suppressed, as shown previously in Sec. III (Fig. 2). Besides, the values of the turn angle are significantly shifted compared to the bulk element. For dysprosium epitaxial films between yttrium layers, it is always larger than the bulk value, whereas it is smaller for dysprosium films between erbium layers. From this result it seems that, in epitaxial layers, the shift of the turn angle from the bulk value is related to the sign of the α epitaxial strains. Moreover, this shift is observed even at high temperature, near the Néel temperature, where the magnetoelastic effects are negligible; it could be therefore explained by a modification of the exchange energy, due to modifications of the Fermi surface of dysprosium by the epitaxial strains. According to the above relation (3), the difference between exchange energies is reduced in the Er/Dy/Er trilayers compared to the bulk and at the opposite, it is enhanced in Y/Dy/Y trilayers.

The determination of the turn angle in the superlattices is more difficult because of the splitting of the satellites due to the sampling by the super-periodicity. It requires a fit of the neutron diffraction spectra, involving, because of the coherence through erbium, two parameters: the wave vector κ_{Dy} of the helical phase in dysprosium and the wave vector κ_{Er} of the spin-density wave in erbium. The total scattered intensities are calculated from the formula (2) presented in Sec. III, with

$$f^{\pm}_{\mathrm{mag}}(\mathbf{q}) = p_{\mathrm{Dy}}\left(\frac{\sin[N(\Lambda q \pm \phi)/2]}{\sin[(\Lambda q \pm \phi)/2]}\right) \times\left(\frac{\sin[(q \pm \kappa_{\mathrm{Dy}})n_{\mathrm{Dy}}c_{\mathrm{Dy}}/2]}{\sin[(q \pm \kappa_{\mathrm{Dy}})c_{\mathrm{Dy}}/2]}\right), \quad (4)$$

where $\phi = \kappa_{\mathrm{Dy}} n_{\mathrm{Dy}} c_{\mathrm{Dy}} + \kappa_{\mathrm{Er}} n_{\mathrm{Er}} c_{\mathrm{Er}}$ and p_{Dy} is the magnetic scattering amplitude proportional to the dysprosium moment component perpendicular to the scattering vector. The magnetic scattering amplitude of erbium does not appear in this formula, which is used above the temperature where erbium presents in-plane magnetic components. The c parameter, concentration, and turn angle profiles have been supposed to be rectangle-wave modulated.

The effective turn angle in the erbium layers determined by the fit is independent of the temperature and approximately equal to the maximum of the generalized susceptibility of the conduction electrons in bulk erbium. The turn angle between dysprosium moments determined by the fit are given in Fig. 18 for several superlattices.

As in bulk material and trilayers, the turn angle between dysprosium moments in Dy/Er superlattices decreases with the temperature. However, the turn angles measured in Dy/Er superlattices are larger than the values measured in bulk dysprosium. This shift is opposite to that observed in Er/Dy/Er trilayers. It indicates that the epitaxial strains are not the sole factor in determining the wave vector of dysprosium in a superlattice; it leads to the conclusion that the superperiodicity may also be about to modify the Fermi surface of dysprosium, and therefore the exchange energy. Moreover, the shift of ω to higher values in the superlattices reveals that the exchange energy of the ferromagnetic phase is increased compared to the energy of the modulated phase, and could partly explain why the Curie temperature in the Dy/Er superlattices is not enhanced, as in Er/Dy/Er trilayers.

VII. DISCUSSION AND CONCLUSION

In summary, we have presented an experimental study of the magnetic behavior of dysprosium in the Dy/Er system. This system appears to be quite complex for intrinsic rea-

sons: both elements are magnetic, exhibit different anisotropy, and develop various magnetic phases strongly related to magnetostrictive effects. The magnetic phases are the result of different contributions to the energy: exchange, anisotropy, and magnetoelasticity. These contributions are about to be modified by the superperiodicity and by the epitaxy. Concerning the epitaxy, it is necessary to consider on one hand, the clamping between the two lattices (e-clamping) and on the other hand, the influence of epitaxial strains.

Besides, the samples are complex composite systems constituted of a thick substrate (1000 times thicker than the layers), a niobium layer, a yttrium (or erbium) buffer, and finally the superlattice (or trilayer) covered by a yttrium (or erbium) cap layer. To conduct a proper and complete study, it should be necessary, but highly difficult, to consider such a sample as a whole. Despite the complexity of the samples, a number of very interesting conclusions can be drawn.

Magnetic phases in the Dy/Er superlattices

In Dy/Er superlattices, when dysprosium is helimagnetic and erbium is paramagnetic, the helix of dysprosium propagates coherently through erbium. The effective turn angle in erbium layers is close to that found in bulk erbium at the ordering temperature. It is remarkable that no sign of ordering of the erbium moments has been observed at a temperature above bulk erbium Néel temperature. The coherence of the helical order is lost for erbium thickness larger than 100 Å.

At a temperature T_C smaller than the Curie temperature of bulk element, dysprosium exhibits a ferromagnetic transition in the layers. The transition is only partial: the helical phase does not completely disappear, even at the lowest temperature.

The relative contribution of the ferromagnetic phase compared to the residual helical order increases with the thickness of the individual dysprosium layers. It does not seem to depend on the yttrium buffer (which indeed is about to stabilize the helical phase) or on the erbium buffer whose effect would be opposite.

At low temperature, the ferromagnetic dysprosium layers are coupled antiferromagnetically to each other, except if the individual erbium layer thickness is smaller than 20 Å. In this case, the long-range magnetic order is ferromagnetic. The long-range antiferromagnetic order observed for erbium thickness larger than 20 Å and the remaining helix are irreversibly destroyed by a 2 kOe field applied in the plane of the sample. The in-plane magnetic component of erbium appears at about 50 K, that is at temperature close to the temperature measured in bulk erbium.

Ferromagnetic transition in trilayers and superlattices

Curie temperature

The epitaxial strains are determinant for the Curie temperature of dysprosium in trilayers. When the dysprosium lattice is constrained in the basal plane (epitaxy on erbium), the ferromagnetic phase is stabilized. When it is expanded (epitaxy on yttrium), the helical phase is stabilized. This is consistent with previous observations on the Lu_xY_{1-x}/Dy/Lu_xY_{1-x} trilayers[15] and can be related to magnetostrictive effects, as it has been shown for dysprosium epitaxial films in considering the total energy of the system, modified by the epitaxial strains.[12–27]

However, the results obtained in Dy/Er superlattices are not in agreement with this simple rule. Indeed contrarily to what happens in the Er/Dy/Er trilayers, the Curie temperatures of dysprosium in Dy/Er superlattices, in which dysprosium should be similarly strained, are lower than in bulk dysprosium. It seems that it should be necessary to consider the magnetic structure of the superlattice as a whole: the energy for an individual dysprosium layer may favor the ferromagnetic phase, whereas the total energy of the whole superlattice may favor the helical arrangement. The helical ordering in dysprosium, which is coherent across several bilayers, may indeed be stable because the conduction electrons form then a coherent spin-density wave in both materials.

Exchange energy

In trilayers, the turn angle seems to be related to the sign of the epitaxial strains: when the dysprosium lattice is constrained in the basal plane (epitaxy on erbium), the turn angle is smaller than in the bulk element, and therefore the difference between the exchange energies of the helical phase and the ferromagnetic phase is lowered. When the lattice is expanded in the basal plane (epitaxy on yttrium), the turn angle is larger, and therefore this difference is increased. These modifications can be due to modifications of the Fermi surface induced by epitaxy and are consistent with the observed shift of the Curie temperature. Exchange and magnetoelastic energies act in the same direction in stabilizing the ferromagnetic phase in dysprosium layers whose basal planes are compressed.

In Dy/Er superlattices, the turn angle between dysprosium moments in the helical phase is larger than in bulk dysprosium, which is unexpected from the trilayers behavior. It means that the epitaxial strains are not the only point to be taken into account and that superperiodicity effects can be at the origin of an increase of the difference between the exchange energies. It leads to the increase of the turn angle and the stabilization of the modulated phase, which is opposite to what is expected from the magnetostrictive energy.

Magnetostrictive strains

In trilayers, the c-lattice parameter of dysprosium varies with temperature in a similar way to bulk dysprosium: c_{Dy} decreases progressively in the helical phase with decreasing temperature and exhibits a discontinuous step at the ferromagnetic transition (when it occurs). The variation of the c parameter is related to the occurrence of the spontaneous α modes which add to the strong epitaxial α strains already present in the paramagnetic phase and measured at room temperature. On the other hand, the orthorhombic γ distortion is observed below T_C but occurs only progressively.

In superlattices, it seems that there is no γ distortion at low temperature. This absence of γ distortion is still to be explained. The influence of erbium (which alone does not develop any γ distortion) on the thin individual dysprosium layers of the superlattice can be invoked. The absence of γ

strain in the superlattice and its smoothness in the trilayers indicate that this mode is probably not the main driving force to the ferromagnetic transition.

In conclusion, as the ferromagnetic transition in dysprosium is known to be governed by a balance between exchange energy and magnetostrictive effects, the lowering of dysprosium Curie temperature in Dy/Er superlattices, unexpected if we only consider the epitaxial strains, could be explained by (i) the reduction of the magnetoelastic driving force resulting from the clamping of the γ mode and (ii) the enhancement of the difference between the exchange energies in the helical and the ferromagnetic phases resulting from a superperiodicity effect.

If the magnetic properties of both elements involved in the superlattice cannot be separated completely, the magnetic ordering in erbium does not seem to affect the magnetic ordering in dysprosium. For example, the antiparallel arrangement between dysprosium layers has been also observed in the Dy/Lu system[3] where lutetium is nonmagnetic at any temperature. However, the coherence of the magnetic components in erbium through dysprosium could be affected, as it has been observed in Ho/Er superlattices[8] and as it will be presented in a paper devoted to erbium in Dy/Er superlattices. The precise magnetic behavior of erbium in the Dy/Er superlattices is still under investigation. Neutron-scattering experiments have already been performed along a direction of the reciprocal lattice where it is possible to evidence the magnetic component along the *c* axis. Moreover, resonant x-ray magnetic-scattering experiments will be conducted in the near future, in order to separate dysprosium and erbium contributions in choosing the incident x-ray energy at different absorption edges.

ACKNOWLEDGMENTS

The authors would like to acknowledge helpful and valuable discussions with J. J. Rhyne and H. Kaiser.

[1] Gd/Y: J. Kwo, E. M. Gyorgy, D. B. McWhan, M. Hong, F. J. Disalvo, C. Vettier, and J. E. Bower, Phys. Rev. Lett. **55**, 1402 (1985).

[2] Dy/Y: J. J. Rhyne, R. W. Erwin, J. Borchers, S. Sinha, M. B. Salamon, R. Du, and C. P. Flynn, J. Appl. Phys. **61**, 4043 (1987).

[3] Dy/Lu: R. S. Beach, J. A. Borchers, A. Matheny, R. W. Erwin, M. B. Salamon, B. Everitt, K. Pettit, J. J. Rhyne, and C. P. Flynn, Phys. Rev. Lett. **70**, 3502 (1993).

[4] Er/Y: J. A. Borchers, M. B. Salamon, R. W. Erwin, J. J. Rhyne, G. J. Nieuwenhuys, R. R. Du, C. P. Flynn, and R. S. Beach, Phys. Rev. B **44**, 11 814 (1991).

[5] Ho/Y: D. A. Jehan, D. F. McMorrow, D. R. A. Cowley, R. C. C. Ward, M. R. Wells, N. Hagmann, and K. N. Clausen, Phys. Rev. B **48**, 5594 (1993).

[6] Ho/Y-Ho/Lu: D. F. McMorrow, D. A. Jehan, P. P. Swaddling, R. A. Cowley, R. C. C. Ward, M. R. Wells, and K. N. Clausen, Physica B **192**, 150 (1993).

[7] Gd/Dy: R. E. Camley, J. Kwo, M. Hong, and C. L. Chien, Phys. Rev. Lett. **64**, 2703 (1990).

[8] Ho/Er: J. A. Simpson, D. F. McMorrow, R. A. Cowley, D. A. Jehan, R. C. C. Ward, M. R. Wells, and K. N. Clausen, Phys. Rev. Lett. **73**, 1162 (1994).

[9] M. K. Wilkinson, W. C. Koehler, E. O. Wollan, and J. W. Cable, J. Appl. Phys. **32**, 48S (1961).

[10] J. W. Cable, E. O. Wolan, W. C. Koehler, and M. K. Wilkinson, Phys. Rev. **140**, A1896 (1965).

[11] D. Gibbs, J. Bohr, J. D. Axe, D. E. Moncton, and K. L. D'Amico, Phys. Rev. B **34**, 8182 (1986).

[12] K. Dumesnil, C. Dufour, Ph. Mangin, G. Marchal, and M. Hennion, Europhys. Lett. **31**, 43 (1995).

[13] J. Kwo, M. Hong, and S. Nakahara, Appl. Phys. Lett. **46**, 319 (1986).

[14] J. A. Borchers, M. B. Salamon, R. W. Erwin, J. J. Rhyne, R. R. Du, and C. P. Flynn, Phys. Rev. B **43**, 3123 (1991).

[15] F. Tsui and C. P. Flynn, Phys. Rev. Lett. **71**, 1462 (1993).

[16] M. B. Salamon, S. Sinha, J. J. Rhyne, J. E. Cunningham, R. W. Erwin, J. Borchers, and C. P. Flynn, Phys. Rev. Lett. **56**, 259 (1986).

[17] W. T. Lee, H. Kaiser, J. J. Rhyne, K. Dumesnil, C. Dufour, Ph. Mangin, G. Marchal, R. W. Erwin, and J. A. Borchers, J. Appl. Phys. **75**, 6477 (1994).

[18] M. Hong, R. M. Fleming, J. Kwo, L. F. Schneemeyer, J. V. Waszczak, J. P. Mannaerts, C. F. Majkrzak, D. Gibbs, and J. Bohr, J. Appl. Phys. **61**, 4052 (1987).

[19] K. Dumesnil, C. Dufour, M. Vergnat, G. Marchal, Ph. Mangin, M. Hennion, W. T. Lee, H. Kaiser, and J. J. Rhyne, Phys. Rev. B **49**, 12 274 (1994).

[20] K. Dumesnil, C. Dufour, Ph. Mangin, G. Marchal, M. Hennion, H. Kaiser, and J. J. Rhyne, J. Magn. Magn. Mater. **140-144**, 775 (1995).

[21] D. R. Behrendt, S. Legvold, and F. H. Spedding, Phys. Rev. **109**, 1544 (1958).

[22] W. E. Evenson and S. H. Liu, Phys. Rev. **178**, 783 (1969).

[23] F. J. Darnell, Phys. Rev. **130**, 1825 (1963).

[24] H. B. Callen and E. Callen, Phys. Rev. **139**, A455 (1965).

[25] J. J. Rhyne and S. Legvold, Phys. Rev. **140**, A2143 (1965).

[26] R. W. Erwin, J. J. Rhyne, M. B. Salamon, J. Borchers, S. Sinha, R. Du, J. E. Cunningham, and C. P. Flynn, Phys. Rev. B **35**, 6808 (1987).

[27] K. Dumesnil, C. Dufour, Ph. Mangin, and G. Marchal, Phys. Rev. B **53**, 11 218 (1996).